Medical Engineering and Physics 92 (2021) 1–9

Contents lists available at ScienceDirect

Medical Engineering and Physics

journal homepage: www.elsevier.com/locate/medengphy

The importance of inertial measurement unit placement in assessing upper limb motion

Gustav Höglund*, Helena Grip, Fredrik Öhberg

Department of Radiation Sciences, Biomedical Engineering, Umeå University, Umeå, Sweden

ARTICLE INFO

Article history:
Received 21 July 2020
Revised 12 February 2021
Accepted 29 March 2021

Keywords:
Motion analysis
Inertial measurement unit
Sensor placement
Measurement protocol
Healthy induviduals
Forearm
Upper arm
Scapula

ABSTRACT

Motion analysis using inertial measurement units (IMU) has emerged as an alternative to optical motion capture. However, the validity and reliability of upper limb measurements varies significantly between studies. The objective of this study was to determine how sensor placement affects kinematic output in the assessment of motion of the arm, shoulder, and scapula. IMUs were placed proximally/distally on arms, and medially/laterally on the scapula, in a group of eleven healthy participants, while performing nine different motion tasks. Linear regressions and mixed models analysed how these different sensor placements affected the estimated joint motion by establishing the linear relationship between sensors placed on the same body segment.

The placement of sensors affected the measured kinematic output considerably, most prominent affect was seen for sensor placement on scapula during flexion and abduction, and on forearm during pronation/supination. The slope of the linear regression lines was 2.5 during flexion, 2.7 during abduction, and 1.8 for forearm pronation/supination. The results of this study suggest that the forearm sensor should be placed on the dorsal side of the forearm, at the distal end; the upper arm sensor should be placed laterally, on the distal part of the arm; and the sensor on the scapula should be placed cranially, along the spine of scapula.

1. Introduction

Motion analysis has the potential to provide an objective, accurate and more detailed way to assess upper limb pathology. Optical skin-based marker systems are considered the gold standard for motion analysis, but they require the remittance of patients to a clinical movement laboratory [1]. Inertial measurement units (IMUs), consisting of gyroscopes, accelerometers and magnetometers [2] are an alternative that can be used in ordinary clinics, since they require only wearable IMU-sensors and a computer where data are registered and analysed. Comparing sensor-based systems with optical systems, recent studies show promising results regarding validity [3] and inter-system agreement [4]. However, as recently reviewed, limited conclusions of the validity and reliability for upper limb motion can be made due to the small number of studies made for each joint [5]. Furthermore, the clinical use of IMUs is limited due to the lack of standardized and validated kinematic protocols [6].

Lack of standardization of biomechanical models, calibration procedures and sensor placements makes it impossible to identify the main source of measurement errors, which causes a high variability between studies [5]. Another reason for inconclusive results related to kinematic analysis of the upper body is the complex anatomy in many of the upper body joints, including the spine and shoulder complexes, which requires standardized placement of the sensors.

Shoulder motion is often approximated with the movement of the upper arm relative to the upper thorax, but is in fact a combination of the acromioclavicular, glenohumeral and scapuloclavicular joints that both rotates and translates. Such simplifications are valid when studying, for example, arm swing during gait [7], but may be too simple when analysing more complex kinematics, such as scapular movement [8]. For example, the analysis of scapular dysfunction is important in obstetrical brachial plexus palsy (OBPP) patients where damage to one or more nerves forming the brachial plexus during birth causes an imbalance in the muscular forces acting on the scapula [9]. Although the majority fully recover, 20 to 30% of effected children suffer from persistent symptoms to a vary-

* Corresponding author.
E-mail addresses: Helena.Grip@umu.se (H. Grip), Fredrik.Ohberg@umu.se (F. Öhberg).

https://doi.org/10.1016/j.medengphy.2021.03.010

Table 1
Study participants.

ID	Sex (M/F)	Age (Y)	Weight (KG)	Height (CM)	Dominant arm (R/L)	Length Upper arm (CM)	Length forearm (CM)
1	M	23	81	183	L	34	28
2	F	23	70	175	R	32	26
3	M	24	85	180	R	33	30
4	F	27	57	168	R	32	26
5	M	25	70	178	L	33	28
6	F	28	67	173	R	33	26
7	M	24	65	180	R	32	28
8	M	24	85	195	R	37	33
9	M	29	88	178	R	31	28
10	F	34	74	171	R	32	27
11	F	46	69	172	R	30	26

M = Male, *F* = Female, *Y* = Years, KG = Kilogram, CM = centimeter, *R* = Right, *L* = Left.

ing degree [10], including muscle weakness, contractures and bone deformities [11], requiring long-term treatment and follow-up. To make decisions regarding different treatment alternatives (surgery, physiotherapy, or botulinum toxin type *A* injections [11]) and to evaluate the treatment outcome, different observational methods, such as the Modified Mallet scale [12] and Active moment scale [13] are used. The scales grade movement function during a set of arm motion tasks and although the scales are highly reliable [14], they have other weaknesses as observational methods. One such weakness is that an observed change in shoulder function may not impact the outcome score [15]. Another weakness is the scales' failure to take into account how upper body joints are coordinated during the motion tasks [16]. A kinematic analysis of upper body function, based on the Mallet scale, may therefore strengthen the clinical assessment of OBPP patients. To be able to implement this in clinic, a protocol based on portable sensors must be validated.

To our knowledge, few or no studies have investigated how IMU sensor placement affects kinematic variables during upper limb motion measurements. We hypothesized that the kinematic variables from the sensor is position dependent due to artefacts from muscle contractions and skin movements but also due to the complexity of joint anatomy. The objective of this study was therefore to evaluate the effect on kinematic variables from distal and proximal sensor placements on arms, and from lateral and medial placements on the scapula, in a group of healthy individuals, while performing standardized arm movements included in the modified Mallet scale.

2. Methods

2.1. Participants

The study group consisted of five female and six male participants with a mean age of 28 ± 6.5 years (see *demographics* in Table 1). One exclusion criterion was the presence of impairment in upper-limb range of motion. Participants were recruited among staff of the Department of Biomedical Engineering at the University Hospital of Umeå and among the student body of Umeå University. Written, informed consent was obtained from all participants prior to inclusion. The study was approved by the Swedish Ethical Review authority (Dnr 09–20 M, supplemented with Dnr 201–232–32 M).

2.2. Equipment

Motion was assessed by a portable movement-analysis system, including seven IMU sensors (MoLab^{TM}, AnyMo AB, Umeå, Sweden). Each sensor contained a three-dimensional gyroscope (16-bit, range ±2000°/s), a three-dimensional accelerometer (16-bit, range ±16 g) and a three-dimensional magnetometer (13-bit, range ±1200 μT). The sample frequency was set to 100 Hz, and data were sent wirelessly to a laptop (Dell Latitude 7400, Intel i5, 8 GB ram). The system was validated for shoulder and elbow motion in previous studies, showing high within-subject reliability for selected outcome variables, and high accuracy in angular data, compared to optical motion capture systems, with a systematic error of a few degrees [17,18].

2.3. Test procedure

The sensors were placed as follows: one sensor on sternum; two on the right scapula; two on the right upper arm; and two on the right forearm (see Fig. 1). The medial scapula sensor was placed cranial to the spine of scapula, at its 1/3 medial portion, and the lateral was placed on the flat surface of acromion. On the upper arm, the proximal sensor was placed centered on the lateral side of the upper arm, and the distal was placed at the distal part of the arm, at a distance from the elbow joint corresponding to one third of the arm's length. The proximal forearm sensor was placed centered on the dorsal side of the forearm, and the distal sensor was placed dorsally at the distal end, close to the ulnar process. Sensors placed on the scapula and sternum were attached with double-sided surgical tape, and the arm sensors were fixed using elastic Velcro straps (Fig. 1).

To prevent magnetic disturbance from affecting the magnetometers in the IMU sensors, participants sat on a wooden chair. The test procedure was standardized and carried out by the same medical student. It consisted of nine arm-movement tasks based on the Modified Mallet Scale [12] (Table 2), with the exception that 'external rotation' was replaced by 'shoulder internal-external rotation'. In addition, standardized range of motion measurements were performed: 'shoulder flexion-extension,' 'elbow flexion-extension.' and 'forearm pronation- supination'. All tasks were repeated five times with the right arm. Each task began with the right arm in neutral position, defined here as the arm hanging vertically, alongside the participant, with the palm of the hand pointing medially. Before each new task, the participant received verbal instruction and a physical demonstration of how to perform the required movement.

2.4. Joint angle definitions

Motion of the scapulothoracic (*Scapula*), humerothoracic (*Shoulder*) and elbow (*Elbow*) joint were analysed. The anatomical coordinate system was defined according to recommendations from the International Society of Biomechanics (ISB) [19]. *Scapula* and *Shoulder* joint angles were defined by the motion of the scapula and upper arm respectively, relative to the thorax. Two different joint angles were analysed for each joint; elevation (Fig. 2a and b) and rotation (Fig. 2c). 'Elevation' was defined as the angle of

Fig. 1. Sensor placement.

Table 2
Task description.

Task	*Description*	*Type of task*	*Motion assessed*
Shoulder FE	Maximal flexion and extension in the sagittal plane, straight arm.	Single plane	Scapula: elevation, Shoulder: elevation
Shoulder AB	Maximal abduction in the frontal plane, straight arm.	Single plane	Shoulder: elevation, Shoulder: elevation
Shoulder ROT	Maximal internal and external rotation, elbows bent to 90°, upper arms along the thorax.	Single plane	Shoulder: rotation
Elbow FE	Maximal flexion and extension in the sagittal plane.	Single plane	Elbow: flexion-extension
Forearm PS	Maximal pronation and supination, elbows bent to 90°, upper arms along the thorax.	Single plane	Elbow: pronation-supination
Hand-to-neck	Placing the hand on the back of the neck.	Compound task	Scapula: elevation and rotation, shoulder: elevation and rotation, elbow: flexion-extension and pronation-supination
Hand-to-spine	Placing the back of the hand on the back, as superiorly as possible.	Compound task	Scapula: elevation and rotation, shoulder: elevation and rotation, elbow: flexion-extension and pronation-supination
Hand-to-mouth	Placing the fingers on the mouth.	Compound task	Scapula: elevation and rotation, shoulder: elevation and rotation, elbow: flexion-extension and pronation-supination
Hand-to-belly	Placing the hand on the belly.	Compound task	Scapula: elevation and rotation, shoulder: elevation and rotation, elbow: flexion-extension and pronation-supination

FE: Flexion-extension, AB: Abduction-adduction, ROT: Internal-external rotation, PS: Pronation-supination, Scapula: Scapulothoracal joint, Shoulder: Humerothoracal joint, Elbow: Elbow joint.

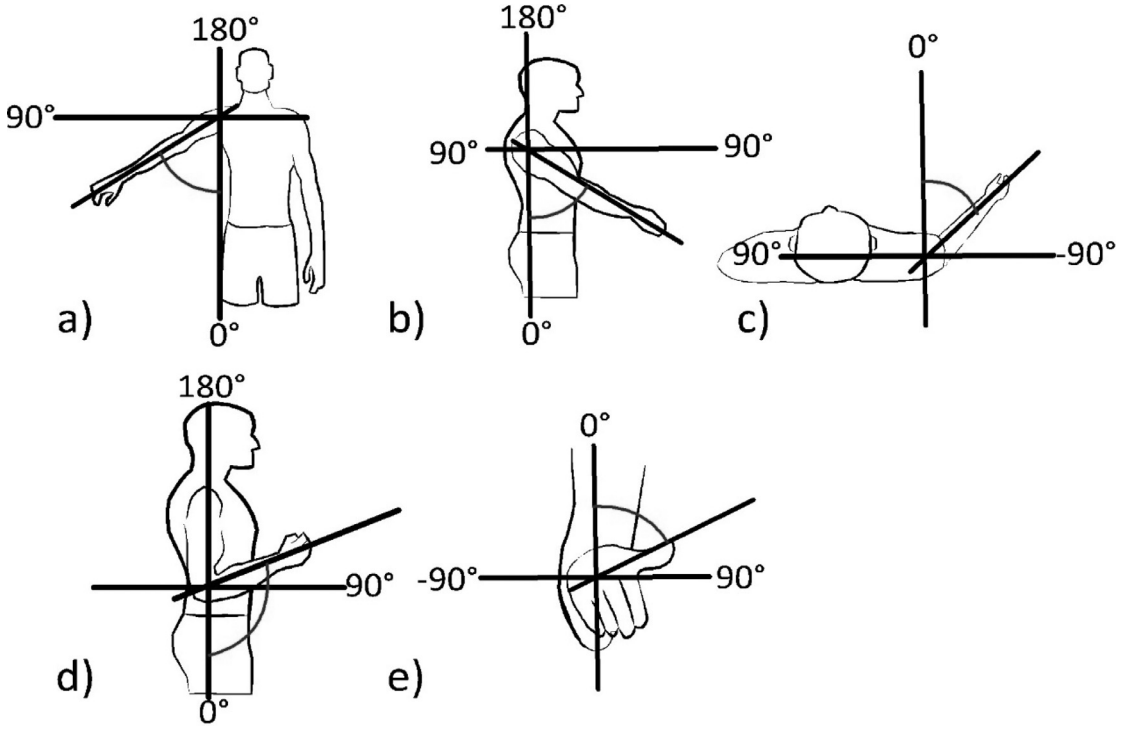

Fig. 2. Analyzed planes/rotation axis. a-b: elevation c: rotation d: flexion-extension e: pronation-supination.

the moving segment's (scapula or upper arm) long axis relative to the long axis of the reference segment (i.e., thorax). 'Rotation' was defined as the angle between the moving segment relative to the thorax in the transversal plane. These angular conventions were selected to avoid gimbal lock, occasionally observed during use of the Euler sequence [20]. Motion in the *Elbow* joint (Fig. 2d and e) was defined as the rotation of the forearm relative to the proximal upper arm sensor, and the Cardan sequence XYZ was used to describe flexion-extension (X) and pronation-supination (Z). Five tasks, 'shoulder flexion-extension', 'shoulder abduction-adduction', 'shoulder internal-external rotation', 'elbow flexion-extension' and 'forearm pronation-supination' were considered to occur in a single plane, and the motion was therefore only analysed in one plane during each task. The other tasks were considered compound and analysed in two planes of motion: rotation and elevation for *Shoulder* and *Scapula* joints and flexion-extension (X) and pronation-supination (Z) for the *Elbow* joint (Table 2). Because two IMU sensors were placed on each segment two sets of joint angles were simultaneously obtained for each of the three defined joints.

2.5. Data analysis and statistics

The sensor data were pre-processed using the MoLab^{TM} analysis software, in which raw data from the gyroscope, accelerometer and magnetometer were combined through a fusion algorithm into joint angles [21], where the filter gain β (i.e., a parameter controlling the amount by which the accelerometer and magnetometer correct the orientation estimated by the gyroscope) was set to 0.03. Each repetition was defined by the time interval that began when the arm started its movement and ended when the arm returned to its initial position. These events were set manually after visual inspection of the kinematic curves and the animated skeleton model. Kinematic data was then time-normalized between two successive events and exported for further statistical analysis. The software IBM SPSS Statistic (version 26, IBM Corp., Armonk, NY, USA) were used for all statistical analyses. The linear relationship between time-normalized data from the proximal/medial and distal/lateral sensor for each task and segment were analysed by a linear regression, where the slope of the regression line and the coefficient of determination (R^2-value) were calculated.

To further analyze the relationship between sensor placement and kinematic output, and to handle the repeated nature of the collected data, a linear mixed model analysis was carried out for each joint and task. In analysing the single plane tasks, the angular data calculated from the distal/lateral sensor was set as the dependent variable, the angular data from the proximal/medial sensor was set as a fixed independent covariate, and study person was used as random intercept. In analysing compound tasks, *Plane* (rotation and elevation for *Scapula* and *Shoulder* joints, flexion-extension and supination-pronation for *Elbow* joint) was used for splitting the analysis into two separate analyses, i.e., one for each plane. A Type-III test of fixed effects was used for testing, where there was a significant fixed independent covariate (i.e., if it deviates from zero).

The estimation method used for finding parameters that describe the fixed effect (i.e., independent covariate) and covariance structure (set to variance components) was the restricted maximum likelihood (REML). The alpha value was set to 0.05 for all statistical tests. To assess the normality assumption, scatter plots of residuals were examined to assess homoscedasticity and normality.

3. Results

Measurement data were collected from all eleven participants. Data from the task 'hand-to-spine' were excluded for one participant, due to poor calibration. Scatter plots, together with the results of the linear regression and R^2-values for the single plane and compound tasks, are illustrated by Figs. 3 and 4, respectively. The type-III test showed a significant fixed independent covariate ($p < 0{,}001$) for all tasks (i.e., both single plane and compound). Results from the analysis of the estimated fixed effect of linear mixed models are presented in Table 3 for the single plane tasks, and Table 4 for the compound tasks.

3.1. Scapulothoracal joint

For the *Scapula* joint, 'shoulder flexion-extension' and 'shoulder abduction-adduction,' slopes of the linear regressions were 2.5 and 2.7, with R^2-values of 0.88 and 0.84, respectively. The same tasks showed an estimated fixed effect of 2.56 (2.55–2.58) and 1.92 (1.90–1.94). For the compound tasks, the elevation measurements had linear regression slopes ranging from 0.9 for 'hand-to-belly' to 2.6 for 'hand-to-neck,' which presented the highest R^2-value, 0.85. Results from 'hand-to-neck' also had the highest fixed effect, 2.89 (2.87–2.91).

Results for the compound tasks showed linear regression slopes between 0.7 and 1.3, and R^2-values ranging between 0.13 and 0.86 for motion in rotation plane. The largest slope (1.3), and R^2-value (0.86), were obtained in 'hand-to-spine'.

3.2. Humerothoracal joint

The linear regression showed slopes of 1.1, and R^2-values of 1.00, for both single plane tasks ('shoulder flexion-extension' and 'shoulder abduction-adduction') which measured motion in the elevation plane. The fixed effects were 1.07 (1.07–1.08) for 'shoulder flexion-extension,' and 1.06 (1.06–1.06), for 'shoulder abduction-adduction'. The obtained linear regression slope was 0.6 in 'hand-to-belly,' with a R^2-value of 0.59, for motion in the elevation plane. The other compound tasks showed linear regression slopes ranging between 1.0 and 1.3 for elevation in the *Shoulder* joint, and presented R^2-values between, 0.98 and 1.00. The fixed effect was 0,57 (0.56–0.58) for 'hand-to-belly,' and ranged between 0.95 (0.95–0.96) and 1.31 (1.30–1.31) for the other compound tasks.

Motion in the rotation plane showed a linear regression slope of 1.4, a R^2-value of 0.94, and a fixed effect of 1.45 (1.44–1.45) for the single plane task 'shoulder internal-external rotation.' The compound tasks showed regression slopes ranging between 1.0 and 1.2, with R^2-values between 0.79 and 0.87. The fixed effects of motion in the rotation plane were smallest in 'hand-to-mouth' 0.97 (0.96–0.98) and largest in 'hand-to-belly,' at 1.39 (1.38–1.40).

3.3. Elbow joint

'Elbow flexion-extension' showed a linear regression slope of 1.0, R^2-value of 0.94, and a fixed effect of 1.04 (1.04–1.04). Linear regression slopes for flexion-extension motion in the *Elbow* ranged, for the compound tasks, between 1.0 and 1.2, with R^2-values of 0.93 to 0.99. The compound task showed fixed effects between 1.01 (1.01–1.01), in 'hand-to-mouth,' and 1.25 (1.24–1.26) in 'hand-to-spine.'

Pronation-supination motion in the single plane task 'forearm pronation-supination' had a linear regression slope of 1.8, a R^2-value of 0.91 and a fixed effect of 1.86 (1.85–1.86). The same motion had linear regression slopes ranging from 0.6 to 1.2, R^2-values between 0.20 and 0.87, and fixed effects ranging between 0.55 (0.53–0.57) and 1.18 (1.17–1.19). 'Hand-to-spine,' which had the highest R^2-value for pronation-supination of the compound tasks (0.87), showed both the largest slope (1.2) and fixed effect 1.18 (1.17–1.19).

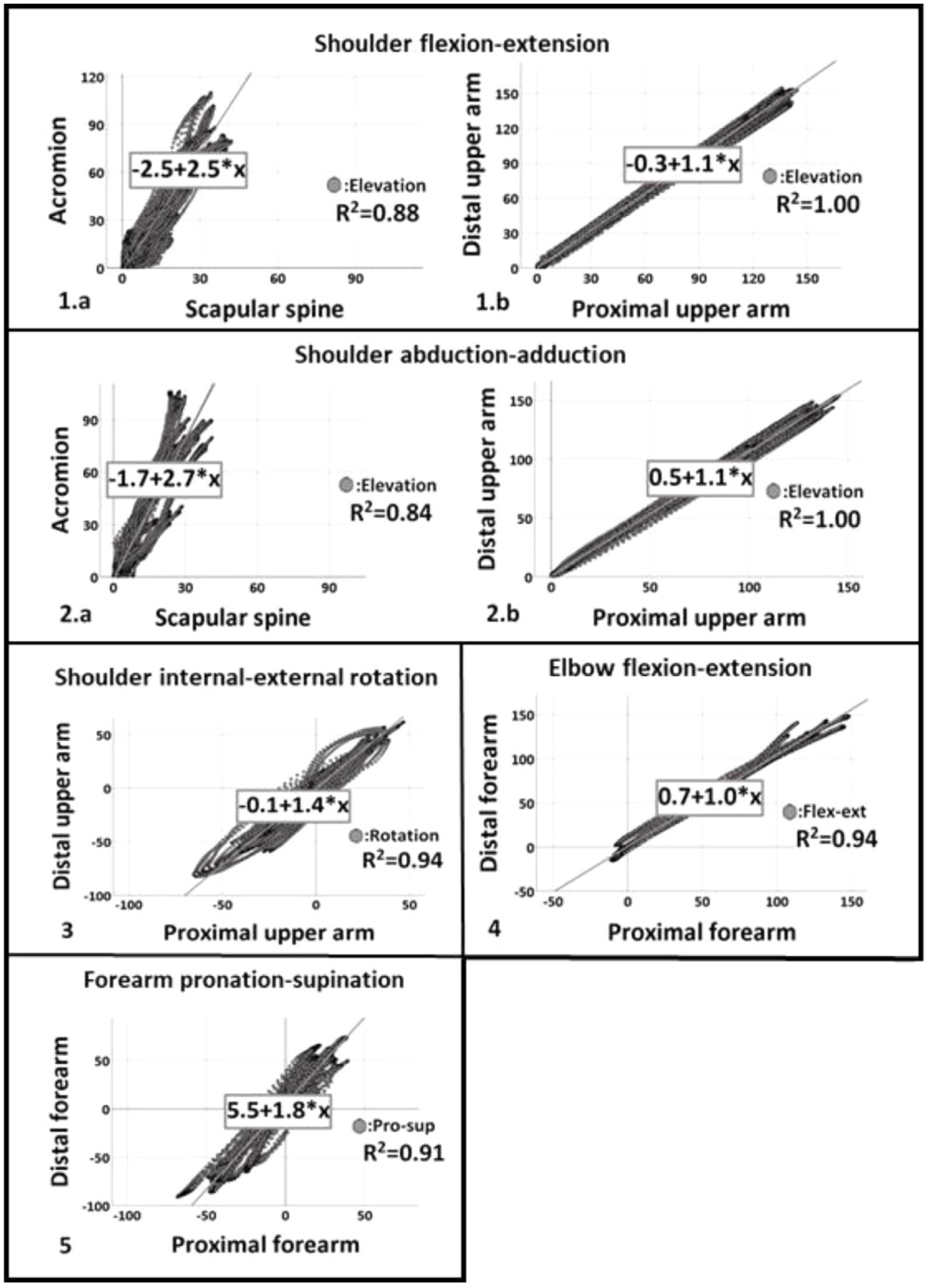

Fig. 3. Scatter plot, linear regression, and R^2-value for single plane tasks. Angles in degrees. 1a-b: Flexion-extension, 2a-b: Abduction-adduction, 3: Shoulder internal external rotation, 4: Elbow flexion-extension, 5: Pronation supination. Flex-ext: Flexion-extension, Pro-sup: Pronation-supination. P-values for linear regression analysis was below 0.001 for all tasks.

4. Discussion

The purpose of this study was to investigate the importance of IMU sensor placement when performing upper limb tasks commonly used in the evaluation of individuals with OBPP. Although soft tissue artefact is an established source of measurement error during non-invasive motion analysis [22], and although sensor placement is known to influence the magnitude of this soft tissue artefact [23], no studies have been made investigating the importance of IMU sensor placement on upper limb motion measurements. The results of this study show that sensor placement has a considerable effect on motion measurement, which could explain the inconclusive validity and reliability reported for measurements of upper limb motion using sensor-based systems in previous studies [5].

Results showed a stronger linear relationship, with higher R^2-values for the single plane tasks when compared to compound tasks. This result is in line with the review made by Poitras et.al [5], which concluded that the validity of IMU measurements decreased with task complexity. Apart from motion complexity, the R^2-value obtained differed between the joints analysed, with overall higher R^2-values for *Shoulder* and *Elbow*, when compared with

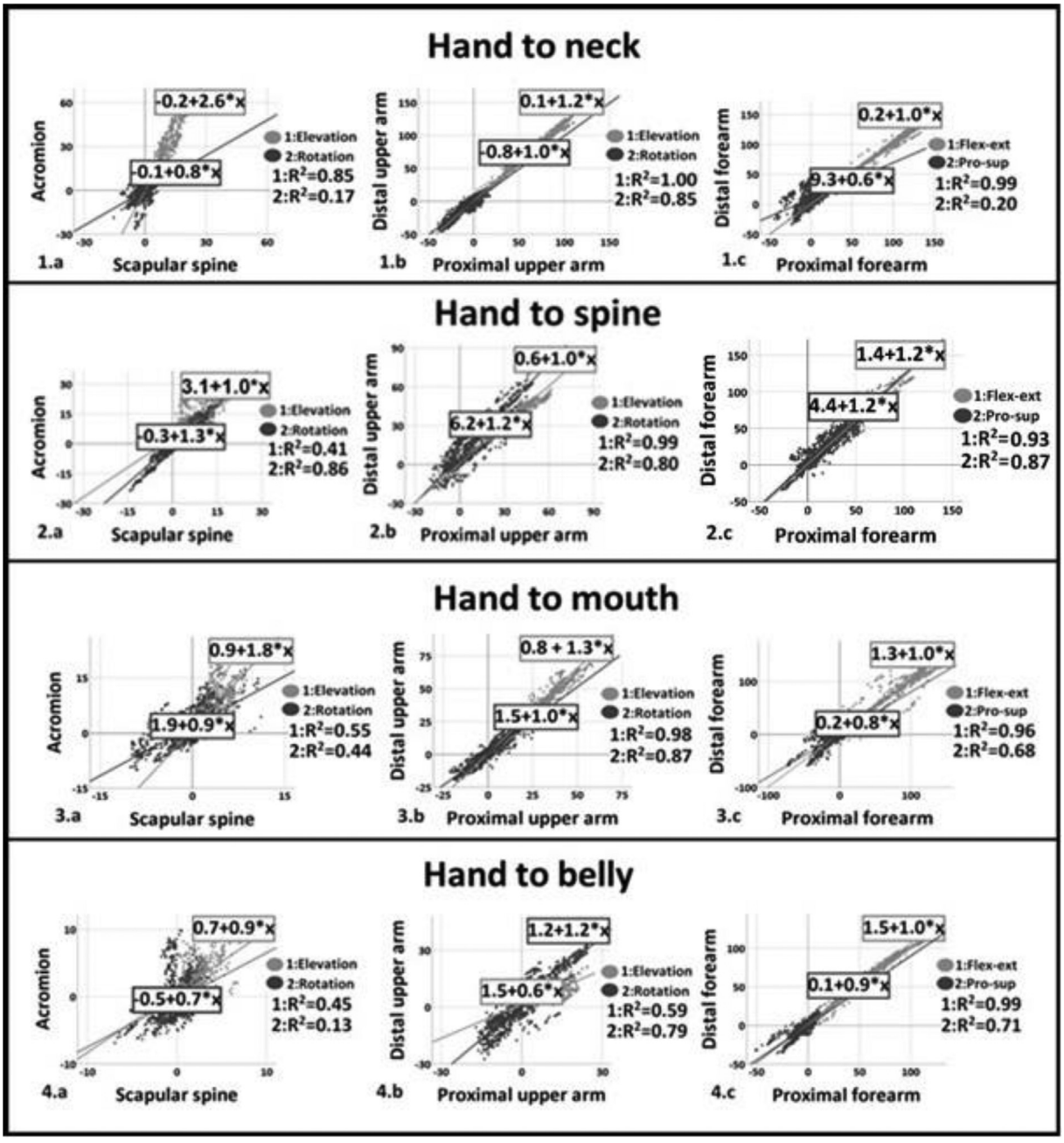

Fig. 4. Scatter plot (10% of all data points), linear regression, and R^2-value for compound tasks. Angles in degrees. 1a–c: Hand-to-neck, 2a–c: Hand-to-spine, 3a–c: Hand-to-mouth, 4a–c: Hand-to-belly. Flex-ext: Flexion-extension, Pro-sup: pronation-supination. *P*-values for linear regression analysis was below 0.001 for all tasks.

Table 3
Mixed model analysis of single plane tasks. Estimated fixed effect of angle derived from distal sensor with angle derived from proximal sensor. Data presented with 95% confidence interval within parentheses.

Task	*n*	*Joint*	*Motion assessed*	*Fixed effect*
Shoulder FE	11,000	Scapula	Elevation	2.56 (2.55–2.58)
		Shoulder	Elevation	1.07 (1.07–1.08)
Shoulder AB	11,000	Scapula	Elevation	1.92 (1.90–1.94)
		Shoulder	Elevation	1.06 (1.06–1.06)
Shoulder ROT	11,000	Shoulder	Rotation	1.45 (1.44- 1.45)
Elbow FE	11,000	Elbow	Flexion-extension	1.04 (1.04–1.04)
Forearm PS	11,000	Elbow	Pronation-supination	1.86 (1.85–1.86)

FE: Flexion-extension, AB: Abduction-adduction, ROT: Internal-external rotation, PS: Pronation-supination, Scapula: Scapulothoracal joint, Shoulder: Humerothoracal joint, Elbow: Elbow joint.

Table 4
Mixed model analysis of compound tasks. Estimated fixed effect of angle derived from distal sensor by analyzed plane and with angle derived from proximal sensor. Data presented with 95% confidence interval within parentheses.

Task	*N*	*Joint*	*Plane 1**	*Plane 2***
Hand-to-neck	22,000	Scapula	2.89 (2.87–2.91)	0.95 (0.92–0.98)
		Shoulder	1.18 (1.18–1.18)	1.11 (1.10–1.12)
		Elbow	1.01 (1.01–1.01)	0.55 (0.53–0.57)
Hand-to-spine	20,000	Scapula	1.31 (1.29–1.34)***	1.20 (1.19–1.21)****
		Shoulder	0.95 (0.95–0.96)	1.25 (1.23–1.26)
		Elbow	1.25 (1.24–1.26)	1.18 (1.17–1.19)
Hand-to-mouth	22,000	Scapula	2.08 (2.05–2.11)	1.05 (1.02–1.09)
		Shoulder	1.31 (1.30–1.31)	0.97 (0.96–0.98)
		Elbow	1.00 (1.00–1.01)	0.81 (0.81–0.82)
Hand-to-belly	22,000	Scapula	0.81 (0.79–0.83)	1.12 (1.10–1.15)
		Shoulder	0.57 (0.56–0.58)	1.39 (1.38–1.40)
		Elbow	1.03 (1.03–1.03)	0.84 (0.83–0.85)

Scapula: Scapulothoracal joint, Shoulder: Humerothoracal joint, Elbow: Elbow joint.
* Elevation for Scapula and Shoulder and flexion-extension for Elbow.
** Rotation for Scapula and Shoulder and pronation-supination for Elbow.
*** No significant interaction type-III test.

Scapula. Another factor, especially prominent in the results from the compound tasks, was the considerably lower R^2-values of tasks with a low range of motion.

4.1. Scapulothoracal joint

Sensor placement had a considerable effect on the measurement of elevation of the *Scapula* joint, during 'shoulder flexion-extension,' and during 'shoulder abduction-adduction.' This can be seen in Fig. 3, where the slope of the regression line was 2.5, and 2.7, respectively, with a R^2-value above 0.8, and in Table 3, where the estimated fixed effect of the angle derived from the distal acromion sensor, with the angle derived from the proximal scapula spina sensor, was 2.56 (2.55–2.58) and 1.92 (1.90–1.94), respectively. 'Hand-to-neck' had a similarly sloped regression line, and an R^2-value similar to the single plane tasks, and considerable higher R^2-value compared with the other compound tasks (Fig. 4). This is also seen in Table 4, where the estimated fixed effect of the angle derived from the distal acromion sensor, with the angle derived from the proximal scapula spina sensor, was 2.89. In addition, the sensor placement had similar effect on the 'hand-to-mouth' task, but with a lower R^2-value (Fig. 4 and Table 4).

Of the measured rotation of the *Scapula* joint during compound tasks, 'hand-to-spine' showed the highest R^2-value, 0.86, and linear regression slope, of 1.3. The other compound tasks presented considerably lower R^2-values (0.13–0.44) (Fig. 4). The results are confirmed in Table 4, where the effect of angle derived from distal sensor, with angle derived from proximal sensor, showed the largest fixed effect, 1.2, for 'hand-to-spine'.

One cause of these results may be interference from the deltoideus muscle over the acromion, which causes the greater range of motion of the sensor placed over acromion. Compared with a study [24] exploring the humeroscapular rhythm using bone pins, the motion of the spina sensor is more in line with their results, and therefore considered to be more accurate and preferable when studying motions of the *Scapula* joint.

4.2. Humerothoracal joint

Results from the single plane tasks showed that sensor placement has relatively little impact on the assessed elevation angle. Seen in Fig. 3 the slope of the regression lines is 1.1 for both, the two tasks showed a very strong linear regression, with R^2-values of 1.00. The same conclusions could be made from the results of the linear mixed model analysis, reported in Table 3, which showed a fixed effect of 1.07 (1.07–1.08) for 'shoulder flexion-extension,' and 1.06 (1.06–1.07) for 'shoulder abduction-adduction'. The slope of the linear regression of the compound tasks, in Fig. 4, showed results similar to the single plane task for tasks 'hand-to-neck' (1.2), 'hand-to-spine' (1.0), and, to some extent, 'hand-to-mouth' (1.3), all of which had high R^2-values, ranging between 0.98 and 1.00. 'Hand-to-belly' differed considerably, with a slope of 0.6, and a low R^2-value, of 0.59. The same tendencies can be seen in Table 4, where 'hand-to-belly' was the task in which the fixed effect of angle derived from distal sensor, with angle derived from proximal sensor, differed most from the single plane task. The low R^2-value, and divergent result of 'hand-to-belly,' was probably caused by lack of motion in the elevation plane during task performance.

Greater importance of sensor placement for *Shoulder* joint motion could be seen in the rotation plane. For the single plane task 'Shoulder internal-external rotation,' seen in Fig. 3, the slope of the regression line was 1.4, R^2-value was 0.94, and the estimated fixed effect of the angle derived from the distal upper arm sensor, with the angle derived from the proximal upper arm, was 1.45 (1.44–1.45) (Table 3). As seen in Fig. 4, the compound tasks 'hand-to-spine,' and 'hand to belly,' showed larger motion in the distal sensor, with slopes of 1.2 for both tasks, and R^2-values of 0.80 and 0.79, respectively. This can also be seen in Table 4, where the fixed effect of 'hand-to-spine' was 1.25 (1.23–1.25) and 1.39 (1.38–1.40). The suspected cause of the modest impact of sensor placement, in the other tasks, is thought to be the lack of motion in the rotation plane.

The smaller range of motion for the proximal sensor is thought to be due to greater soft tissue interference. This suggests that more distal sensor placement would be preferable to more proximal placement. Furthermore, the greater importance of upper arm sensor placement for measurements in the rotation plane might explain the high variability of validity for IMU measurements for shoulder rotation, compared to shoulder flexion and abduction, seen in the review by Poitras et al. [5].

4.3. Elbow joint

Seen in Fig. 3, *Elbow* joint showed no effect of the distal sensor, relative to the proximal, with a linear regression slope of 1.0, and a high R^2-value of 0.94 for 'elbow flexion-extension.' A modest impact was seen for the task in the linear mixed model analysis, Table 3, with a fixed effect of 1.04 (1.04–1.04). *Elbow* flexion-extension showed, like the single plane task, no effect of sensor placement on the regression line in all compound tasks, except

for 'hand-to-spine,' R^2-values were between 0.93–0.99 (Fig. 4). Like the single plane task, a small impact from sensor placement was seen in the compound tasks (Table 4) except 'hand-to-spine,' which showed a fixed effect of 1.25 (1.24–1–26).

Greater impact from sensor placement could be seen in the *Elbow* joint for pronation-supination. The single plane task 'forearm pronation-supination,' showed a regression slope of 1.8 (R^2-value of 0.91), as seen in Fig. 3, and in Table 3, where the fixed effect was 1.86 (1.85–1.86). This result differed substantially from the results of *Elbow* joint pronation-supination in the compound tasks, as seen in Fig. 4, where slopes range from 0.6 to 1.2, with R^2-values between 0.2 and 0.87; and in Table 4, where fixed effects range between 0.55 (CI95 0.53–0.57) and 1.18 (CI95 1.17–1.19). This divergence between the single plane tasks, and compound tasks, is thought to be due to sensor crosstalk (i.e., an error involving misaligned axes during sensor placement), also mentioned by Groves [25]. The larger range of motion for the distal sensor in the 'forearm pronation-supination' task is assumed less due to soft tissue intervention, than the greater distance from the joint's center of rotation.

4.4. Strengths and limitations

Both strengths and limitations can be noted in this study. One weakness is the limited participant cohort of 11 included participants, without any known disability in the upper body. The altered motion pattern of individuals diagnosed with OBPP is well known [26] and this might influence the outcome from different sensor placements in another way than in healthy individuals. Furthermore, the importance of sensor placement was evaluated by the comparison of measurements from two sensors, rather than establishing the actual accuracy of the system. Also, the source of the measurement discrepancy between different sensor placements was not investigated. The sensor crosstalk believed to affect the angular results from the *Elbow* joint (i.e. pronation-supination motion in the compound tasks), might have been prevented if another calibration method had been used. Ligorio et al. [27] presented a functional calibration method, where crosstalk for supination pronation was equal to the crosstalk seen with an optical reference system.

The study's strengths include the use of the same test leader to conduct all tests, and the use of a predefined measurement protocol. This prevented possible interrater discrepancy. Another strength was the concurrent assessment of measurement from all sensors, gathered from the same motion at the same time.

4.5. Clinical implications

The result of this study implicates that a standardized protocol, including standardized sensor placement, is essential for reliable upper body motion analysis. Sensor placement on the flat surface of the acromion had a large effect on angular measurements of the *Scapula* joint, as compared to placement cranial to the spine of the scapula. This is most likely due to large movements of the deltoid muscle that occur during elevation of the shoulder, which cause the sensor to increase its elevation more than the movement of scapula. The sensor placement seemed to have little importance for *Shoulder* motion in the elevation plane, but considerable effect when measuring motion in the rotation plane. The difference in the assessed angle in the rotation plane is probably caused by the effect of greater soft tissue, over the central portions of the upper arm, on the proximal sensor. When analysing the *Elbow*, the sensor placement was important in 'pronation supination' motion direction, which is natural, since the rotation is larger in the distal end of the arm, compared to the proximal end, due to restrictions on how the radius and ulna are attached to the proximal radioulnar joint. Flexion-extension was less affected by sensor placement, since the humeroulnar joint is a hinge-joint that allows for flexion and extension only, thereby affecting the sensors equally, since they are placed along an approximately straight line.

Based on the results from this study, certain single plane tasks, e.g., *Shoulder* flexion-extension, abduction-adduction, and *Elbow* flexion-extension, can be especially recommended for repeated clinical measurements, since they are less affected by sensor placement. In single plane tasks, e.g., *Shoulder* internal-external rotation, where sensor placement had a greater influence on the assessed angle, placement should be well considered and documented to obtain accurate and reliable clinical measurements. As mentioned earlier, the impact of sensor placement on compound tasks showed broader and less predictable influence of motion measurements. The added value of objective motion measurements for these tasks should be considered, if used clinically. Objective measurements of joint movements, in connection with single plane and compound movements, do not appear to provide greater added value as merely measuring the single plane movements. Nevertheless, in the study of strategies for task achievement, objective measurements of compound tasks could prove valuable to future studies, and have clinical implications. We also believe that objective measurements of joints in the upper extremities will provide information crucial for the long-term measurement of daily life activities.

5. Conclusion

In summary, sensor placement affects the obtained kinematic output differently, depending on the analysed joint and plane of rotation. The placement of sensors on the scapula considerably affected the measured kinematic output during flexion and abduction, and on the forearm during pronation and supination. To reduce the influence of underlying muscle and skin movements, our results recommend the following placement of motion sensors: On the dorsal side, at the distal end of the forearm (i.e., as close to the ulnar process as possible); the upper arm sensor, laterally, on the distal part of the arm; and the scapula sensor, cranially, along the spine of the scapula.

Declaration of Competing Interest

None

Fredrik Öhberg and Helena Grip are shareholders of the company AnyMo AB, which is manufacturing both sensors and analysis software used in this study.

Ethical approval: The study was approved by the Swedish Ethical Review authority (Dnr 09–20 M, supplemented with Dnr 201–232–32 M).

Founding: This work was founded by the University Hospital of Umeå and Sweden's innovation agency VINNOVA.

References

[1] Morrow MMB, Lowndes B, Fortune E, Kaufman KR, Hallbeck MS. Validation of inertial measurement units for upper body kinematics. J Appl Biomech 2017;33:227–32. doi:10.1123/jab.2016-0120.

[2] Filippeschi A, Schmitz N, Miezal M, Bleser G, Ruffaldi E, Stricker D. Survey of motion tracking methods based on inertial sensors: a focus on upper limb human motion. Sensors 2017;17. doi:10.3390/s17061257.

[3] Cutti AG, Giovanardi A, Rocchi L, Davalli A, Sacchetti R. Ambulatory measurement of shoulder and elbow kinematics through inertial and magnetic sensors. Med Biol Eng Comput 2008;46:169–78. doi:10.1007/s11517-007-0296-5.

[4] Parel I, Cutti AG, Kraszewski A, Verni G, Hillstrom H, Kontaxis A. Intra-protocol repeatability and inter-protocol agreement for the analysis of scapulo-humeral coordination. Med Biol Eng Comput 2014;52:271–82. doi:10.1007/s11517-013-1121-y.

[5] Poitras I, Dupuis F, Bielmann M, Campeau-Lecours A, Mercier C, Bouyer LJ, et al. Validity and reliability of wearable sensors for joint angle estimation: a systematic review. Sensors 2019;19. doi:10.3390/s19071555.

[6] Petuskey K, Bagley A, Abdala E, James MA, Rab G. Upper extremity kinematics during functional activities: three-dimensional studies in a normal pediatric population. Gait Posture 2007;25:573–9. doi:10.1016/j.gaitpost.2006.06.006.
[7] Goudriaan M, Jonkers I, van Dieen JH, Bruijn SM. Arm swing in human walking: what is their drive? Gait Posture 2014;40:321–6. doi:10.1016/j.gaitpost.2014.04.204.
[8] Lempereur M, Brochard S, Leboeuf F, Remy-Neris O. Validity and reliability of 3D marker based scapular motion analysis: a systematic review. J Biomech 2014;47:2219–30. doi:10.1016/j.jbiomech.2014.04.028.
[9] Raducha JE, Cohen B, Blood T, Katarincic J. A review of brachial plexus birth palsy: injury and rehabilitation. R I Med J 2017;100(2013):17–21.
[10] Malessy MJ, Pondaag W. Obstetric brachial plexus injuries. Neurosurg Clin N Am 2009;20:1–14 v. doi:10.1016/j.nec.2008.07.024.
[11] O'Berry P, Brown M, Phillips L, Evans SH. Obstetrical brachial plexus palsy. Curr Probl Pediatr Adolesc Health Care 2017;47:151–5. doi:10.1016/j.cppeds.2017.06.003.
[12] Abzug JM, Chafetz RS, Gaughan JP, Ashworth S, Kozin SH. Shoulder function after medial approach and derotational humeral osteotomy in patients with brachial plexus birth palsy. J Pediatr Orthop 2010;30:469–74. doi:10.1097/BPO.0b013e3181df8604.
[13] Curtis C, Stephens D, Clarke HM, Andrews D. The active movement scale: an evaluative tool for infants with obstetrical brachial plexus palsy. J Hand Surg Am 2002;27:470–8. doi:10.1053/jhsu.2002.32965.
[14] Bae DS, Waters PM, Zurakowski D. Reliability of three classification systems measuring active motion in brachial plexus birth palsy. J Bone Joint Surg Am 2003;85:1733–8. doi:10.2106/00004623-200309000-00012.
[15] Bialocerkowski AE, Wrigley T, Galea M. Reliability of the V-scope system in the measurement of arm movement in children with obstetric brachial plexus palsy. Dev Med Child Neurol 2006;48:913–17. doi:10.1017/s001216220600199x.
[16] Mahon J, Malone A, Kiernan D, Meldrum D. Reliability of 3D upper limb motion analysis in children with obstetric brachial plexus palsy. Physiol Meas 2017;38:524–38. doi:10.1088/1361-6579/aa5c13.
[17] Ertzgaard P, Ohberg F, Gerdle B, Grip H. A new way of assessing arm function in activity using kinematic exposure variation analysis and portable inertial sensors–a validity study. Man Ther 2016;21:241–9. doi:10.1016/j.math.2015.09.004.
[18] Ohberg F, Backlund T, Sundstrom N, Grip H. Portable sensors add reliable kinematic measures to the assessment of upper extremity function. Sensors 2019;19. doi:10.3390/s19051241.
[19] Wu G, van der Helm FC, Veeger HE, Makhsous M, Van Roy P, Anglin C, et al. ISB recommendation on definitions of joint coordinate systems of various joints for the reporting of human joint motion–part II: shoulder, elbow, wrist and hand. J Biomech 2005;38:981–92. doi:10.1016/j.jbiomech.2004.05.042.
[20] Senk M, Cheze L. Rotation sequence as an important factor in shoulder kinematics. Clin Biomech 2006;21(Suppl 1):S3–8 Avon. doi:10.1016/j.clinbiomech.2005.09.007.
[21] Madgwick SO, Harrison AJ, Vaidyanathan A. Estimation of IMU and MARG orientation using a gradient descent algorithm. IEEE Int Conf Rehabil Robot 2011;2011:5975346. doi:10.1109/ICORR.2011.5975346.
[22] Li JD, Lu TW, Lin CC, Kuo MY, Hsu HC, Shen WC. Soft tissue artefacts of skin markers on the lower limb during cycling: effects of joint angles and pedal resistance. J Biomech 2017;62:27–38. doi:10.1016/j.jbiomech.2017.03.018.
[23] Stagni R, Fantozzi S, Cappello A, Leardini A. Quantification of soft tissue artefact in motion analysis by combining 3D fluoroscopy and stereophotogrammetry: a study on two subjects. Clin Biomech 2005;20:320–9 Avon. doi:10.1016/j.clinbiomech.2004.11.012.
[24] Ludewig PM, Phadke V, Braman JP, Hassett DR, Cieminski CJ, LaPrade RF. Motion of the shoulder complex during multiplanar humeral elevation. J Bone Joint Surg Am 2009;91:378–89. doi:10.2106/jbjs.g.01483.
[25] Groves PD. Navigation using inertial sensors [Tutorial]. IEEE Aerosp Electron Syst Mag 2015;30:42–69. doi:10.1109/maes.2014.130191.
[26] Russo SA, Kozin SH, Zlotolow DA, Thomas KF, Hulbert RL, Mattson JM, et al. Scapulothoracic and glenohumeral contributions to motion in children with brachial plexus birth palsy. J Shoulder Elbow Surg 2014;23:327–38. doi:10.1016/j.jse.2013.06.023.
[27] Ligorio G, Zanotto D, Sabatini AM, Agrawal SK. A novel functional calibration method for real-time elbow joint angles estimation with magnetic-inertial sensors. J Biomech 2017;54:106–10. doi:10.1016/j.jbiomech.2017.01.024.